HHS Public Access

Author manuscript

Biomaterials. Author manuscript; available in PMC 2016 April 07.

Published in final edited form as:

Biomaterials. 2010 February ; 31(4): 680–690. doi:10.1016/j.biomaterials.2009.09.092.

Surfaces modified with nanometer-thick silver-impregnated polymeric films that kill bacteria but support growth of mammalian cells

Ankit Agarwal[a], **Tahlia L. Weis**[b], **Michael J. Schurr**[b], **Nancy G. Faith**[c], **Charles J. Czuprynski**[c], **Jonathan F. McAnulty**[d], **Christopher J. Murphy**[d,**], and **Nicholas L. Abbott**[a,*]

[a]Department of Chemical and Biological Engineering, University of Wisconsin-Madison, WI 53706, USA

[b]Department of Surgery, School of Medicine and Public Health, University of Wisconsin-Madison, USA

[c]Department of Pathobiological Sciences, School of Veterinary Medicine, University of Wisconsin-Madison, USA

[d]Department of Surgery, School of Veterinary Medicine, University of Wisconsin-Madison, USA

Abstract

Silver is widely used as a biocidal agent in ointments and wound dressings. However, it has also been associated with tissue toxicity and impaired healing. *In vitro* characterization has also revealed that typical loadings of silver employed in ointments and dressings (~ 100 μg/cm^2) lead to cytotoxicity. In this paper, we report the results of an initial study that sought to determine if localization of carefully controlled loadings of silver nanoparticles within molecularly thin films immobilized on surfaces can lead to antimicrobial activity without inducing cytotoxicity. Polymeric thin films of poly(allylamine hydrochloride) (PAH) and poly(acrylic acid) (PAA) were prepared by layer-by-layer deposition and loaded with ~0.4 μg/cm^2 to ~23.6 μg/cm^2 of silver nanoparticles. Bacterial killing efficiencies of the silver-loaded films were investigated against *Staphylococcus epidermidis*, a gram-positive bacterium, and it was determined that as little as ~0.4 μg/cm^2 of silver in the polymeric films caused a reduction of 6 $\log_{10}$ CFU/mL (99.9999%) bacteria in suspensions incubated in contact with the films (water-borne assays). Significantly, whereas the antibacterial films containing high loadings of silver were found to be toxic to a murine fibroblast cell line (NIH-3T3), the polymeric films containing ~0.4 μg/cm^2 of silver were not toxic and allowed attachment, and growth of the mammalian cells. Thus, the results of this study go beyond prior reports by identifying silver-impregnated, polymeric thin films that are compatible with *in vitro* mammalian cell culture yet exhibit antibacterial activity. These results

*Corresponding author: Current address: School of Veterinary Medicine, Surgical and Radiological Sciences, 1423 Tupper Hall, University of California at Davis, Davis, CA 95616-8745, USA, abbott@engr.wisc.edu (N.L. Abbott). **Corresponding author. Current address: School of Veterinary Medicine, Surgical and Radiological Sciences, 1423 Tupper Hall, University of California at Davis, Davis, CA 95616-8745, USA, cjmurphy@ucdavis.edu (C.J. Murphy).

Appendix: Figure with essential colour discrimination. Many of the figures in this article have parts that are difficult to interpret in black and white. The full colour images can be found in the on-line version, at doi:10.1016/j.biomaterials.2009.09.092.

Appendix. Supplementary data: Supplementary material associated with this paper can be found, in the online version, at doi:10.1016/j.biomaterials.2009.09.092

support the hypothesis that localization of carefully controlled loadings of silver nanoparticles within molecularly thin polymeric films can lead to antimicrobial activity without cytotoxicity. More broadly, this strategy of modifying surfaces with minimal loadings of bioactive molecules indicates the basis of approaches that may permit management of microbial burden in wound beds without impairment of wound healing.

Keywords

Silver nanoparticles; Wound healing; Wound-bed engineering; Nanostructured polymer films; Antibacterial activity; Cytotoxicity

1. Introduction

Silver is a non-specific biocidal agent that acts against a broad spectrum of bacterial [1], and fungal [2] species, including several antibiotic resistant strains [3]. Silver-based compounds and formulations have been used to treat burn wounds for centuries [3– 5], particularly for the prevention of burn wound sepsis [4–7]. The antimicrobial efficacy of topical silver has encouraged the development of several silver-functionalized ‘active’ wound care dressings [5,8,9]. In these approaches, the dressings serve as macroscopic reservoirs of high concentrations of silver. The silver is eluted from the dressing and transported by diffusion to the surface of the wound bed to establish antimicrobial activity [8]. The highly reactive nature of silver ions make them susceptible to inactivation by proteins and chloride ions within the complex environment defined by wound fluid [10–12], contributing to the need for high concentrations of silver ions in these topical delivery systems [8]. An alternative approach has been to perform frequent dressings changes to the wound, but this approach is often painful for patients and it is costly [13].

The above-described standard approaches for delivery of silver to wound beds typically lead to large excesses of silver being delivered to the wounds and surrounding tissue. This excess silver can have detrimental effects. For example, silver ions have been reported to accumulate in epithelial cells, macrophages, fibroblasts and connective tissue [4,12] and they have been shown to cause tissue toxicity and impaired wound healing [5,7,14]. *In vitro* studies have also demonstrated that the concentrations of silver ions incorporated into wound healing products can be cytotoxic to mammalian cells involved in wound healing, including fibroblasts [15–17], keratinocytes [15] and lymphocytes [18]. One recent study reported rapid induction of differential cell death by all the leading silver dressings that were tested *in vitro* [19], while another study reported elevation of hepatic enzymes and argyria-like symptoms in burn patients treated with a leading silver dressing [14]. In summary, although silver is clearly an effective antimicrobial agent, it also leads to dose-related toxicity in tissue. In particular, when diffused to the surface of a wound bed from a macroscopic silver reservoir such as a dressing or ointment, the high loadings and concentrations of silver necessary to establish antimicrobial activity in the wound bed are not well-controlled and can become cytotoxic and impair wound healing [5,20,21].

In the study described in this paper, we report the results of an initial investigation aimed at developing principles that can overcome the above-described limitations of current silver

delivery systems. We test the hypothesis that nanoscopic localization of precisely-defined loadings of silver on a surface can lead to antimicrobial activity without inducing cytotoxicity. This hypothesis is based on the proposition that localization of silver on a surface can generate the concentrations of silver required for antimicrobial activity at the surface (Fig. 1a) without requiring the high loading of silver that is typically required to drive mass transport of silver from a macroscopic reservoir to the surface (Fig. 1b). Our approach employs molecularly thin polymeric films to localize silver nanoparticles on surfaces. The films are prepared by using 'layer-by-layer' assembly of oppositely charged polyelectrolytes [22]. These polyelectrolyte multilayers (PEMs) are comprised of interpenetrating polymeric layers, with typical thicknesses in the 10–100 nm range [23,24]. Their porous and supramolecular architectures allow incorporation of a variety of molecules including DNA, proteins, viruses, inorganic colloids, and organic dyes [23]. Because PEMs can conformally coat a range of different types of surfaces, including the surfaces of biological and synthetic materials [24], they can potentially be prepared *in situ* on a wound-bed, pre-assembled and transferred from flexible sheeting material to a wound bed, or used to functionalize implantable medical devices.

Several past studies have reported the preparation of PEMs that contain silver and display antibacterial activity by releasing silver into solution [25–29]. In particular, Rubner and coworkers [30–32] demonstrated that PEMs formed from weak polyacids of poly(allylamine hydrochloride) (PAH) and poly(acrylic acid) (PAA) can incorporate metallic cations such as Ag^+ from solution (Fig. 2). The Ag^+ ions were incorporated into the PEMs via ion exchange with the acidic protons of the PAA and subsequently reduced to zerovalent Ag nanoparticles by using an aqueous solution of a chemical reducing agent. Because the number of free carboxylic acid groups of PAA within the PEMs that were available for ion exchange with Ag^+ was controlled by varying the pH of the PAA solution during assembly of the PEM, these past studies have established that the loading of silver within PEMs can be manipulated by varying the pH of the assembly solution. These past studies have also characterized the size, volume fraction and concentration of silver nanoparticles [33] in the films. Of particular relevance to this paper, films with loadings of silver nanoparticles of $\sim$5.5 μg/cm^2 or more were prepared, and shown to exhibit antibacterial activity [31,33]. However, neither the minimum loading of silver required for antibacterial activity nor the interactions of mammalian cells with the silver nanoparticle-loaded PEMs (including cytotoxicity) were reported. We do note that several prior studies have investigated adhesion and spreading of mammalian cells on PEMs not containing silver nanoparticles [34,35]. These studies revealed that PEMs of PAA and PAH, when prepared under conditions identical to those used previously to prepare silver-loaded PEMs [25,26], swelled substantially and did not permit attachment and growth of mammalian cells [34].

We end this introduction by noting that a past study by Shi et al has reported on silver-loaded PEMs prepared from a polymer containing quaternary ammonium ions [29]. For a single loading of silver nanoparticles within the PEMs, they reported antimicrobial activity and compatibility with mammalian cell culture. In that study, however, the PEMs exhibited antimicrobial activity in the absence of silver. In our study, we have used polymers that do not exhibit antibacterial activity, and thus we can attribute the antimicrobial activity of the PEMs to the presence of the silver.

2. Materials and methods

2.1. Preparation of polyelectrolyte multilayer (PEM) films

The positively charged polyelectrolyte PAH (Mw = 70 kDa, Sigma Aldrich, St. Louis, MO) and the negatively charged polyelectrolyte PAA (Mw = 90 kDa, Polysciences, Warrington, PA) were used to prepare the PEMs. Silver nitrate and the reducing agent sodium borohydride ($NaBH_4$) from Sigma Aldrich (St. Louis, MO) were used for the synthesis of the silver nanoparticles within the PEMs. Deionized water (18.2 MΩ cm) was used to prepare all aqueous solutions. Fluorescein isothiocyanate-labeled PAH (FITC-PAH), Mw 70 kDa, was prepared using FITC (Invitrogen, Carlsbad, CA) as described elsewhere [36].

PEMs were assembled on glass coverslips (5 mm diameter) that were cleaned by plasma oxidation (using PlasmaTherm 1441 RIE Instrument (8 sccm O_2, 300 s, 100 W)). Aqueous solutions of PAA and PAH (0.01 M by repeat unit), adjusted to the desired pH using either 1 M HCL or 1 M NaOH, were used to prepare the PEMs. The plasma oxidized glass coverslips (5 mm diameter) were placed at the bottom of the wells of a 96-well plate (BD Falcon® Polystyrene, non-tissue culture treated 96-well plates, BD, Franklin Lakes, NJ), and PEMs were assembled by sequentially placing solutions of either PAH or PAA in the wells for 10 min. The formation of the PEMs was initiated by the adsorption of PAH onto the glass coverslips. After incubation of a coverslip against a given polyelectrolyte solution, the solution in the well was exchanged three times with water (2 min each; water adjusted to pH 5.5 using HCl) to remove free polyelectrolyte from the well [36]. This process of sequential polyelectrolyte adsorption and rinsing was repeated to obtain the desired number of polyelectrolyte bilayers. A bilayer here is defined as one layer of PAH plus one layer of PAA. After assembly, the PEM films were dried in vacuum at 60 °C for 1 h.

Synthesis of the silver nanoparticles (Ag NPs) within the PEMs was initiated by incubation of the pre-assembled PEMs (see above) in an aqueous solution of silver nitrate (5 mM) at pH 7.0 (adjusted with 0.01 N HNO_3) for 1 h. As described previously, Ag^+ ions diffuse into the PEMs and exchange with the acidic protons of the PAA [31,32]. The carboxylate-bound Ag^+within the PEMs were subsequently reduced to zero-valent Ag NPs by incubation of the PEMs (dried in vacuum oven at 60° C for 1 h) in 1 mM $NaBH_4$ aqueous solution (pH 7.0) for 15 min [33]. In addition to forming the Ag NPs, this procedure regenerates the carboxylic acid groups within the PEMs. This permits additional Ag^+ to be loaded into the PEMs. Thus, repeated cycles of incubation in Ag^+ solutions and then reducing agent can be used to increase the loading of Ag NPs in the PEMs.

The loading of silver incorporated into the PEMs was determined by dissolving the silver nanoparticles in the PEMs into 100 μl diluted nitric acid for 30 min. The concentration of Ag^+ extracted from the PEMs was measured (after suitable dilution into a 5 mL solution of dilute nitric acid) by elemental analysis using an inductively-coupled plasma (ICP) emission spectrometer (Perkin Elmer Optima 3000DV) at $\lambda_{328.068}$ [29]. The detection limit of the instrument was specified to be ~0.1 ppb. See Supplementary Materials for details regarding the analytical method.

2.2. In vitro cytotoxicity assay

The mouse fibroblast cell line NIH-3T3, obtained from ATCC (Manassas, VA), was used for all *in vitro* cell-based experiments. Cell cultures were maintained in a humidified environment with 5% CO_2 at 37 °C and were fed with DMEM growth medium supplemented with 10% calf bovine serum (CBS) and 1 μM L-glutamine (Invitrogen, Carlsbad, CA). For cell culture, PEM-coated glass coverslips housed in 96-well plates were first sterilized with UV irradiation (268 nm) for 15 min and then washed three times with PBS. Cells were seeded with 1.5×10^4 cells/well of the 96-well plate. Controls used were PEM-coated glass coverslips with no silver, and uncoated glass coverslips (plasma oxidized). Cells treated with 1% Triton X-100 (Sigma Aldrich, St Louis, MO) were used as controls for complete cell death. After incubation for 24 h in growth medium, cells were washed with PBS and labeled with fluorescent live/dead assay stains (Invitrogen, #L3224) following the manufacturer's protocol. Briefly, cells were incubated for 30 min with 0.6 μM calcein AM (ex/em ~495 nm/515 nm) and 2 μM ethidium homodimer-1 (EthD-1, ex/em ~495 nm/~635 nm) in PBS buffer. Calcein AM is an intracellular esterase substrate that undergoes a 40-fold increase in fluorescence upon cleavage (fluoresces green) and thus serves as an indicator of the number of live cells present. Ethidium homodimer is excluded from live cells but with loss of viability it enters the cell and binds to DNA upon which it exhibits a marked increase in fluorescence (fluoresces red) and provides an indication of the number of dead cells present. Fluorescence was measured on a Synergy™ multi-mode microplate reader (BioTek Instruments, Winooski, VT) and percentage cell viability and cell death were calculated relative to controls. An Olympus IX70 inverted microscope equipped with Chroma Technology Corp. (Rockingham, VT) fluorescence filter cubes was used to image the cells. Images were captured and analyzed using the Metavue version 7.1.2.0 software package (Molecular Devices, Toronto, Canada).

2.3. Antibacterial activity

The antibacterial activity of silver-impregnated PEMs was determined by incubating a suspension of *Staphylococcus epidermidis* cells in contact with PEM-coated glass coverslips. The strain of *S. epidermidis* used was a clinical isolate from the University of Wisconsin-Madison Veterinary Hospital (provided by Professor R. D. Schultz). *S. epidermidis* was grown in Tryptic Soy Broth Yeast Extract (TSBYE) (BD, Franklin Lakes, NJ) overnight at 37 °C with shaking at 200 rpm until it reached a cell density of approximately 4×10^9 CFU/mL The latter was extrapolated from a standard curve for optical density λ_{600nm}) as measured with a UV-vis spectrometer (Beckman Coulter, Fullerton, CA). The bacterial suspension was centrifuged at 2700 rpm for 10 min and the pellet washed and resuspended in PBS. To test the antibacterial activity of the PEMs, PEM-coated glass coverslips (5 mm diameter) were placed in wells of a 96-well plate and incubated with 10^7 CFU of *S. epidermidis* in 100 μL PBS buffer with shaking (100 rpm) at 37 °C for 8 h. After incubation, buffer from the wells was collected, and the wells (with cover-slips) were washed 3 × in 200 μL ice cold PBS to rinse out any bacteria. For each well, washings were pooled and the final volume was made to 1 mL using PBS. The viable bacterial cells in the collected buffer samples were determined by a surface spread-plate method [25]. Serial dilutions of the samples were prepared in PBS and 0.1 mL of each diluted sample was spread onto Trypticase Soy Blood Agar plates (#221261, BD, Franklin

Lakes, NJ,) and the plates allowed drying. After incubation in a 37 °C incubator for 24 h, bacterial colonies were counted and used to calculate the mean colony forming units (CFU) per mL. All assays were carried out on at least three different days, with three replicates of each test sample every time. The results are reported as the mean ± standard deviation (SD).

2.4. Statistical analyses

Where appropriate, the data is presented as means with standard deviations (SD) as error bars, calculated over three or more data points. Significant difference between two groups were evaluated by Student's *t*-test and between more than two groups by one-way ANOVA analysis of variance, followed by Tukey's test. The level of significance was set at $p < 0.05$.

3. Results

3.1. Biocompatibility of polymer multilayers

The first experiments performed in our study sought to characterize the interactions of mammalian cells with silver-containing PEMs of PAH/PAA that were prepared under conditions reported previously to lead to antimicrobial activity [25,26]. As noted in the Introduction, although these past studies have clearly established that silver-impregnated PEMs can exhibit antimicrobial activity, they have not characterized the interactions of mammalian cells with those silver-loaded PEMs. To this end, PEMs containing 10.5 bilayers of PAH/PAA (i.e. with PAH as the top and bottom layer) were prepared (as described in the Methods section) on glass coverslips (diameter of 5 mm). The PAH was incorporated into the PEMs from solutions at pH 7.5 to ensure that the PAH (with pK_a of ~9.5 [37]) would be protonated; the pH of the PAA solutions used to prepare the PEMs was varied to manipulate the degree of ionization of the PAA (with pK_a of ~5.5 [37]). As previously published [31,33], the capacity of a PEM containing PAA to bind Ag^+ from solution is largely determined by the number of free carboxylic acid groups present in the PAA during the assembly process (and thus is affected by the pH of the PAA solutions used to prepare the PEMs). In this report, we denote the PEMs as PAH/PAA$_x$, where x is the pH of the PAA solution used to assemble the PEMs. Following previous reports, PEMs were initially assembled using PAA solutions with pH values of 2.5, 3.5 or 4.5 [25,26,31–33]. Each set of PEMs was impregnated with silver nanoparticles, as described above, by sequential immersion in a silver nitrate solution and solution of chemical reducing agent. We confirmed formation of the PEMs on the glass coverslips by measurement of cumulative fluorescence of PEMs prepared using a fluorescently labeled PAH (see Supplementary Materials, Fig. 1).

Following fabrication, we characterized the attachment and spreading of NIH-3T3 mouse fibroblast cells on PEMs formed from PAH/PAA$_{2.5,\ 3.5,\ 4.5}$ (both for PEMs containing silver nanoparticles and PEMs free of silver nanoparticles). The cells were seeded on the PEM-coated surfaces in serum-supplemented (10% calf bovine serum (CBS)) growth media and the viability of the cells was determined after 24 h using Calcein-AM (live stain) and ethidium homodimer (dead stain). Fig. 3 shows micrographs of the NIH-3T3 cells on either glass coverslips (no PEM, Fig. 3a), on glass coverslips coated with PEMs that were free of silver (Fig. 3b,d and f), or glass coverslips that were coated with silver-loaded PEMs (Fig. 3c,e and g). Inspection of Fig. 3a reveals that the cells attached and spread on the glass

coverslips (no PEMs), and that the majority of the attached cells were viable (as indicated by staining with Calcein-AM (green), and absence of staining with ethidium homodimer (red)). In contrast, the NIH-3T3 fibroblast cells did not spread on the silver-free PEMs prepared with PAH/$PAA_{2.5}$ (Fig. 3b) [37]. The fibroblasts on these PEMs were rounded and formed clusters (additional micrographs are shown in Supplementary Materials, Fig. S2). The lack of attachment and spreading of cells on these weakly (ionically) cross-linked PEMs is consistent with the prior observations by Mendelsohn et al. [34] who proposed that PEMs formed under these conditions swell and hydrate in buffers, thereby preventing attachment and spreading of fibroblasts (they used NR6WT fibroblasts, a cell line derived from NIH-3T3 cells). Thus, while PEMs containing PAA deposited at pH 2.5 possess a high density of carboxylic acid groups available for binding of silver [31,33], these PEMs do not promote attachment and spreading of fibroblasts. Inspection of Fig. 3b,d and freveals that as the pH of the PAA solution used to prepare the PEMs was increased from 2.5 to 3.5 to 4.5 (i.e. from $PAA_{2.5}$ to $PAA_{4.5}$), the attachment, spreading and viability of fibroblasts cells on the PEMs surface was observed to improve. However, when silver nanoparticles were impregnated within any of these PEMs, almost no live cells were found spread on the PEMs after 24 h incubation, and the majority of cells that were attached were rounded and dead (Fig. 3c,e and g). These results indicate that the silver-containing PEMs, prepared as described above, are cytotoxic to fibroblast cells. We conclude that silver-impregnated PEMs, when prepared as reported previously to exhibit antimicrobial activity, are cytotoxic to mammalian cells (fibroblasts). These initial results led us to consider three key questions. First, what is the loading of silver in the PEMs reported above, and is it possible to manipulate the loading of silver in PEMs formed from PAH and PAA over a broader range than has been reported in the past (see below)? Second, at what loadings of silver do the silver-loaded PEMs no longer exhibit toxicity to mammalian cells? Third, at loadings of silver where PEMs are not toxic to mammalian cells, do the silver loaded PEMs retain their antimicrobial properties? Below we address each of these questions in series.

3.2. Loading of silver in the PEMs

To address the first of the above-posed questions, we sought to measure the loading of silver in the PEMs and to determine if it was possible to manipulate the loading of silver within the PEMs over a broad range. Towards that end, we prepared PEMs from PAH and PAA where the pH of the solution used to assemble the PAA into the PEMs was systematically changed from pH 2.5 (where less than <1% of the acid groups in PAA are ionized) to pH 7.5 (where the extent of ionization of the PAA is >95%) [37]. To determine the loading of silver in the PEMs, silver was extracted from the PEMs into dilute nitric acid and quantified by elemental analysis using an inductively-coupled plasma (ICP) emission spectrometer. By normalizing the amount of silver extracted from the PEMs with the total surface area of the PEMs on the glass coverslips, the loading of silver in the PEMs ($\mu g/cm^2$) was calculated (Fig. 4). These results, including the concentrations of silver released from the PEMs into the dilute nitric acid, are summarized in Table 1 in Supplementary Materials.

It is evident from Fig. 4 that the loading of silver in the PEMs (10.5 bilayers of PAH/PAA) can be tuned from 23.65 ± 1.14 $\mu g/cm^2$ to 0.39 ± 0.03 $\mu g/cm^2$. Inspection of Fig. 4 also reveals that the decrease in loading of silver in the PEMs is subtle when the pH of the PAA

solution used to prepare the PEMs was increased beyond 4.5 (containing 0.63 ± 0.15 μg/cm^2 silver). This trend is presumably caused by the titration behavior of the carboxylic acids of the PAA [30]. In particular, we note that the loading of silver in the PEMs prepared from PAA at pH 4.5 was 0.63 ± 0.15 μg/cm^2, and that those PEMs were shown in Fig. 3g to be cytotoxic to NIH-3T3 fibroblast cells. To our knowledge, PEMs prepared using solutions of PAA with pH values between 4.5 and 7.5, when loaded with silver nanoparticles, have not been investigated previously for antibacterial activity or mammalian cell toxicity. Below, we reveal that the subtle changes in the loading of silver within PEMs shown in Fig. 4 (with pH of PAA solution >4.5) have significant effects on their functional properties (antimicrobial activity and compatibility with mammalian cells).

3.3. Cytotoxicity of silver-impregnated multilayers of PAH/PAA$_{5.5–7.5}$

To test the above-described proposition regarding cytotoxicity of PEMs containing low loadings of silver, we prepared PEMs using PAA assembled from solutions at pH 5.5, 6.5 or 7.5. We first tested the PEMs prepared without silver to confirm that they would permit attachment and spreading of NIH-3T3 cells. Inspection of Fig. 5a,c and e confirms attachment, spreading and viability (Calcein AM stain) of the cells on these silver-free PEMs. Furthermore, these micrographs reveal that the PEMs prepared with PAA at high pH (pH of 7.5) caused the highest levels of spreading of the cells. The attachment, spreading and viability of cells measured on the PEMs of PAH/PAA$_{7.5}$ is comparable to that observed on the glass coverslips (no PEMs; Fig. 3a). Additional images presented in Fig. S3 of Supporting Information confirm spreading of the cells over large areas of these PEMs. Next, we incorporated silver nanoparticles within these PEMs, and investigated the influence of the silver nanoparticles on the culture of NIH-3T3 cells. Inspection of Fig. 5b,d and f leads to several important observations. First, the cells grown on PAH/PAA$_{5.5}$ films impregnated with silver nanoparticles were rounded and contained dead stain. Thus, we conclude that the incorporation of silver into these PEMs leads to cytotoxicity. Second, in contrast to the PEMs denoted PAH/PAA$_{5.5}$, we observed the NIH-3T3 cells to attach, spread and exhibit high levels of viability (green Calcein AM stain) on silver-impregnated PEMs of PAH/PAA$_{6.5}$ and PAH/PAA$_{7.5}$. A significant finding that emerges from this set of experiments is, therefore, that incorporation of silver nanoparticles into the PEMs of PAH/PAA$_{6.5}$ and PAH/PAA$_{7.5}$ does not lead to cytotoxicity (absence of red EthD-1 dead stain). It is also evident that the cells are more uniformly attached and better spread on the silver-impregnated PEMs of PAH/PAA$_{7.5}$ as compared to PAH/PAA$_{6.5}$. Fig. S3 of Supporting Information confirms that these differences in attachment and spreading are seen across large areas of the two different PEMs.

To confirm the above-described qualitative observations, we quantified the percentage of viable cells on the PEMs (relative to untreated glass controls) by measurement of the total fluorescence of the live and dead stains. Fig. 6 shows that almost all of the cells were viable (i.e. contained live stain) when cultured on silver-free, PEM-coated surfaces (prepared using PAA at pHs that ranged from 2.5 to 7.5). This result is an interesting one in light of the result shown in Fig. 3, where the fibroblast cells are shown not to spread on weakly ionically crosslinked PEMs (i.e., those PEMs prepared from PAA solutions at low pH). Taken together, these results suggest that the PEMs themselves are not cytotoxic when prepared

from PAA solutions at low pH, but that they resist attachment and spreading of cells due to their molecular organization and resulting mechanical properties [34,35]. In contrast, when using silver-loaded PEMs, the results in Fig. 6 show that the viability of fibroblasts on the PEMs correlate closely with their silver content, which in turn is governed by the pH at which the PAA was incorporated into the PEMs. In particular, whereas very few live cells were found attached to PEMs of PAH/PAA5.5 containing 0.58 ± 0.04 μg/cm^2 silver, approximately 80% of cells (relative to untreated glass controls) were alive on PEMs of PAH/PAA$_{6.5}$ containing 0.48 ± 0.05 (μg/cm^2 silver, and almost all cells were alive on PEMs of PAH/PAA7.5 containing 0.39 ± 0.03 μg/cm^2 silver. The key conclusion that emerges from the data in Figs. 5 and 6 is that silver-loaded PEMs prepared with PAA at pH 7.5 are compatible with the culture of NIH-3T3 cells (they do not exhibit measurable cytotoxicity). The mechanical properties of these PEMs lead to high levels of attachment and spreading (Fig. 5) and the loadings of silver in these PEMs are sufficiently low that they do not cause cellular toxicity (Fig. 6). Below we provide additional evidence that it is the release of silver from these PEMs that determines the cellular toxicity of the PEMs.

3.4. Cytotoxicity of silver ions in solution

Cytotoxicity of silver to mammalian cells *in vitro* is well documented, with several researchers reporting on the cytotoxic effects of silver ions on fibroblasts [15,16], keratinocytes [15], hepatocytes [38], and lymphocytes [18]. In particular, Hidalgo et al [16] reported that silver nitrate concentrations greater than 2.8 ppm in growth media (supplemented with 10% fetal calf serum) were cytotoxic (greater than 90% cell death in 24 h) to human dermal fibroblasts (obtained from skin biopsies at their hospital). Guided by these prior observations, we sought to determine if the concentrations of silver ions potentially released by the silver-loaded PEMs characterized in Fig. 4 are cytotoxic to NIH-3T3 fibroblasts. To this end, we incubated NIH-3T3 cells in growth media (containing 10% CBS) supplemented with silver nitrate. Fig. 7 shows representative micrographs of NIH-3T3 cells labeled with live and dead fluorescent stains (described in Methods Section) after incubation for 36 h with the silver nitrate-supplemented growth media (note that the NIH-3T3 fibroblast cells were cultured in 100 μL of cell culture media). Inspection of Fig. 7 reveals that silver nitrate was cytotoxic to NIH-3T3 cells at concentrations above 1 ppm, with only 10% live cells (relative to untreated controls) attached to the tissue culture plates incubated for 36 h with 2 ppm silver ions (Fig. 7e), and no live cells (Fig. 7f) on those surfaces incubated with 5 ppm or higher silver ions. These results, when combined with data presented in Fig. 6, lead to several observations. First, the cell death observed on the (PAH/PAA)$_{10}$ multilayers prepared using PAA solutions with pH values below 6.5 (i.e., PEMs containing 0.48 ± 0.05 μg/cm^2 or more of silver) suggests that the PEMs exposed the cells to at least 1 ppm of silver ions in order to trigger the cell death. Second, the cell behaviors observed on the PEMs prepared using solutions of PAA at pH 7.5 (i.e., PEMs containing 0.39 ± 0.03 μg/cm^2 silver), on which all fibroblasts seeded were alive and spread after a 24 h incubation, suggests that the cells on those PEMs were exposed to concentrations of silver that were less than 1 ppm. Indeed, if all silver within the PEMs containing 0.39 ± 0.03 μg/cm^2 of silver was released into the cell culture media, we calculate the concentration of silver in the culture media to be 0.76 ± 0.06 ppm (see Table 1 of Supplementary Data). These results lead us to conclude that these PEMs (prepared using PAA at pH 7.5) are likely

not substantially cytotoxic to fibroblasts because the loading of silver is insufficient to generate toxic concentrations of silver.

3.5. Antimicrobial activity of silver-loaded PEMs that do not exhibit mammalian cell toxicity

Next we sought to determine if PEMs with low loadings of silver (prepared using PAA at high pH) would exhibit levels of antibacterial activity comparable to PEMs reported in the past (which contained high loadings of silver but killed mammalian cells in this study). To this end, we prepared silver-loaded PEMs from PAH/$PAA_{2.5–7.5}$ and tested the PEMs for their bactericidal activity against suspended cells of the gram-positive bacterium *S. epidermidis* (*S. epi.*). In this assay, surfaces presenting silver-loaded PEMs were incubated with 10^7 CFU of *S. epidermidis* in 100 μl PBS buffer, pH 7.4 at 37 °C with shaking (100 rpm) for up to 8 h, after which bacteria were collected in ice-cold PBS and viable cell counts were determined. As controls, bacterial suspension was also incubated with untreated glass surfaces, glass surfaces coated with silver-free PEMs or glass surfaces coated with silver-free PEMs that were treated with the reducing agent (sodium borohydride (1 mm)) used to prepare the silver nanoparticles. The results are presented in Fig. 8. Similar to the bare glass control, we observed no reduction in the viable *S. epidermidis* counts when the bacteria were incubated in contact with surfaces coated with silver-free PEMs, or with silver-free PEMs treated with the reducing agent. In contrast, when bacterial suspension was incubated with silver loaded PEMs of PAH/$PAA_{2.5}$ (containing 23.65 ± 1.14 μg/cm^2 silver), we observed a 6 $\log_{10}$ reduction in CFUs of *S. epidermidis*, i.e. more than 99.9999% of bacteria cell death, as illustrated in Fig. 8a. Silver-loaded PEMs prepared with PAH/$PAA_{3.5,4.5,5.5 \text{ or } 6.5}$ (containing 1.06 ± 0.10, 0.64 ± 0.08, 0.58 ± 0.04, or 0.48 ± 0.05 μg/cm^2 silver, respectively) also exhibited similar levels of antibacterial activity (results not shown). Most significantly, the silver-loaded PEMs that were prepared with PAH/PAA7.5 and contained only 0.39 ± 0.03 μg/cm^2 silver also exhibited similar high levels of antibacterial activity, i.e. a 6 log10 reduction in viable *S. epidermidis*, as illustrated in Fig. 8b. To provide additional evidence that this antibacterial effect is due to silver incorporated into the PEM, we further decreased the loading of silver in the PEMs by reducing the concentration of silver nitrate solution in which PEMs were incubated to impregnate them with silver ions (in the experiments described above, we used 5 mM silver nitrate solutions). The results in Fig. 8b show that as the concentration of silver nitrate solution (in which PEMs prepared with PAH/$PAA_{7.5}$ were incubated) was decreased from 5 mM to 0.5 mM and then 0.05 mM, the resulting silver-loaded PEMs killed 99.99% and 90% of the bacteria, respectively, incubated in contact with the surfaces. When the concentration of silver nitrate used to prepare the PEMs was decreased below 5 μM, the antimicrobial activity of the PEMs was lost. In summary, this dose-response curve confirms the role of the silver in the antimicrobial activity of the PEMs, and demonstrates important finding that there exists a window of silver loadings in the PEMs where the PEMs exhibit antimicrobial activity yet do not cause mammalian cell toxicity (using mouse fibroblasts).

4. Discussion

A key finding of this study is that there exists a range of loadings of silver in PEMs prepared from PAA and PAH that do not lead to mammalian cell toxicity yet do exhibit antimicrobial

activity. This finding was made possible because the loadings of silver within the PEMs could be precisely controlled over a wide range. Whereas past studies have reported manipulation of the loading of silver in PEMs prepared from PAA and PAH between ~ 50 μg/cm^2 and 5 μg/cm^2, we found that the lowest of these loadings of silver still induced cytotoxicity. In order to prepare PEMs that were not toxic to mammalian cells, we found that we needed to lower the loading of silver below 0.4 μg/cm^2. Significantly, at these loadings of silver, the PEMs still exhibited antimicrobial activity.

An important insight into the compatibility of the silver-loaded PEMs used in our study comes from companion measurements in which we examined the cytotoxic effects of soluble silver concentrations. If all the silver within a PEM loaded with 0.4 μg/cm^2 of silver was to dissolve into the cell culture medium used in our studies, we calculate that the concentration of silver in the culture media would be <1 ppm. Inspection of Fig. 6 reveals that this concentration of soluble silver does not lead to cytotoxicity. This result contrasts to a past study by Shi et al. [29], who reported on the toxicity of PEMs containing 25 μg/cm^2 of silver nanoparticles. Although these authors report that their PEMs were compatible with cells for 48 h, data on rates of silver release presented in their report indicate that growth of mammalian cells on these PEMs for times longer than 48 h would lead to levels of soluble silver that would be cytotoxic. A significant point that emerges from our study is that absence of cytotoxicity (with retention of antimicrobial activity) can be achieved by using loadings of silver that are sufficiently low. In contrast, the absence of cytotoxicity in the report by Shi et al. [29] is likely because the silver within the PEM was not fully released to the cell culture media. This difference is significant because higher release rates or longer incubation times can lead to cytotoxic effects in the latter but not the former system.

It is interesting to also compare the loadings of silver in the PEMs prepared from PAH and PAA that lead to antimicrobial activity to the loadings of silver used in silver-based wound treatments. Silver-based topical solutions that are currently used in clinical practice for wound healing, such as 0.5 wt% silver nitrate solution, or ointments such as 1 wt% silver sulfadiazine cream, release silver at concentrations up to 3200 ppm, although most of this silver is thought to be rapidly inactivated through the formation of chemical complexes in the wound [6]. A prototypical example of silver-impregnated wound dressings is Acticoat®. These dressings are designed to provide a sustained release of silver over an extended period of time [19]. Acticoat® contains nanocrystalline silver [6] at a loading of ~100 μg/cm^2 and can release 80–100 ppm of silver in water [1,39]. It has been shown to be cytotoxic to keratinocytes and fibroblasts [14,15] and cause rapid induction of differential cell death programmes in cells *in vitro* [19]. In contrast to these conventional approaches, the silver-loaded PEMs used in the studies reported in this paper contain several orders of magnitude less silver (as low as 0.4 μg/cm^2, releasing a total of 0.76 ± 0.06 ppm silver ions into 100 μl solution), yet they still demonstrate effective antibacterial activity. Furthermore, these silver impregnated PEMs allow attachment and growth of adhesive cells like fibroblasts. Although 3T3 cells cytotoxicity does not directly correlate with impairment of clinical wound healing in humans, the sensitivity of this cell line to silver allowed us to fine tune the dose-related toxicity. Finally, we note that evaluation of the clinical utility of these silver loaded PEMs for wound healing will require characterization of the temporal properties of these systems,

testing of other mammalian cell lines and bacterial strains, and studies in animal models, which will be reported in the future studies.

In summary, our results support the proposition that nanometer-thick polymeric films that permit integration of silver nanoparticles into wound beds will allow precise delivery of therapeutic levels of silver. This precise delivery could lead to the effective control of wound bioburden without silver-related cytotoxicity currently encountered with macroscopic topical silver-delivery agents used for wound healing [5,15,38,40]. More broadly, our results using silver impregnated PEMs support the general concept of nanoscopic localization of bioactive molecules by nanometer thick polymer multilayers. We envision engineering the wound bed with other bioactive agents, such as growth factors and extracellular matrix constituents to optimize wound healing and promote favorable patient outcomes.

5. Conclusion

We demonstrate that precise control of the loading of silver nanoparticles in molecularly thin polymeric films can lead to engineered surfaces that permit attachment and spreading of mammalian cells while also demonstrating antibacterial activity. Results presented in this paper are consistent with the conclusion that the absence of cytotoxicity arises because the loading of silver within the polymeric thin films is insufficient to generate toxic concentrations of silver. This contrasts with currently employed macroscopic strategies (ointments and wound dressings) wherein antimicrobial activity is typically achieved with loadings of silver that can lead to cytotoxicity. The high loadings of silver associated with these conventional approaches to silver-based wound-care are also known to impair wound healing. The results of our study suggest the basis of new approaches for management of microbial burdens in wounds that employ integration of nanoscopic silver and other bioactive agents into wound beds. It serves as the first demonstration of a generalizable approach for the controlled engineering of the wound bed to promote wound healing.

Supplementary Material

Refer to Web version on PubMed Central for supplementary material.

Acknowledgments

We thank Christopher A. Worley at the Water Science and Engineering Laboratory, University of Wisconsin-Madison for technical assistance with the ICP-ES, and Adeyinka A. Lesi for assistance with preparation of the PEMs. The funding for this study was provided by Wisconsin Institute for Discovery.

References

1. Yin HQ, Langford R, Burrell RE. Comparative evaluation of the antimicrobial activity of Acticoat™ antimicrobial barrier dressing. J Burn Care Rehabil. 1999; 20(3):195–200. [PubMed: 10342470]
2. Wright JB, Lam K, Hansen D, Burrell RE. Efficacy of topical silver against fungal burn wound pathogens. Am J Infect Control. 1999; 27(4):344–50. [PubMed: 10433674]
3. Wright JB, Lam K, Burrell RE. Wound management in an era of increasing bacterial antibiotic resistance: a role for topical silver treatment. Am J Infect Control. 1998; 26(6):572–7. [PubMed: 9836841]

4. Klasen HJ. Historical review of the use of silver in the treatment of burns. I. Early uses. Burns. 2000; 26(2):117–30. [PubMed: 10716354]
5. Atiyeh BS, Costagliola M, Hayek SN, Dibo SA. Effect of silver on burn wound infection control and healing: review of the literature. Burns. 2007; 33(2):139–48. [PubMed: 17137719]
6. Dunn K, Edwards-Jones V. The role of Acticoat™ with nanocrystalline silver in the management of burns. Burns. 2004; 30(Suppl. 1):S1–9. [PubMed: 15327800]
7. Cho Lee AR. Effect of silver sulfadiazine on the skin cell proliferation and wound healing process in hairless mouse 2nd degree burn model. J Korean Pharm Sci. 2002; 32:113–7.
8. Mooney EK, Lippitt C, Friedman J. Silver dressings. Plast Reconstr Surg. 2006; 117(2):66, 6–9.
9. Ip M, Lui SL, Poon VKM, Lung I, Burd A. Antimicrobial activities of silver dressings: an in vitro comparison. J Med Microbiol. 2006; 55(1):59–63. [PubMed: 16388031]
10. Maple PAC, Hamilton-Miller JMT, Brumfitt W. Comparison of the in-vitro activities of the topical antimicrobials azelaic acid, nitrofurazone, silver sulphadiazine and mupirocin against methicillin-resistant *Staphylococcus aureus*. J Antimicrob Chemother. 1992; 29(6):661–8. [PubMed: 1506349]
11. Spacciapoli P, Buxton D, Rothstein D, Friden P. Antimicrobial activity of silver nitrate against periodontal pathogens. J Periodont Res. 2001; 36(2):108–13. [PubMed: 11327077]
12. Kristiansen S, Ifversen P, Danscher G. Ultrastructural localization and chemical binding of silver ions in human organotypic skin cultures. Histochem Cell Biol. 2008; 130(1):177–84. [PubMed: 18392636]
13. Sheridan R, Petras L, Lydon M, Salvo P. Once-daily wound cleansing and dressing change: efficacy and cost. J Burn Care Rehabil. 1997; 18(2):139–40. [PubMed: 9095423]
14. Trop M, Novak M, Rodl S, Hellbom B, Kroell W, Goessler W. Silver-coated dressing acticoat caused raised liver enzymes and argyria-like symptoms in burn patient. J Trauma. 2006; 60(3): 648–52. [PubMed: 16531870]
15. Poon VKM, Burd A. In vitro cytotoxity of silver: implication for clinical wound care. Burns. 2004; 30(2):140–7. [PubMed: 15019121]
16. Hidalgo E, Bartolomé R, Barroso C, Moreno A, Domínguez C. Silver nitrate: antimicrobial activity related to cytotoxicity in cultured human fibroblasts. Skin Pharmacol Appl Skin Physiol. 1998; 11(3):140–51. [PubMed: 9745141]
17. Lee AR, Moon HK. Effect of topically applied silver sulfadiazine on fibroblast cell proliferation and biomechanical properties of the wound. Arch Pharm Res. 2003; 26(10):855–60. [PubMed: 14609135]
18. Hussain S, Anner RM, Anner BM. Cysteine protects Na, K-ATPase and isolated human lymphocytes from silver toxicity. Biochem Biophys Res Commun. 1992; 189(3):1444–9. [PubMed: 1336367]
19. Van Den Plas D, De Smet K, Lens D, Sollie P. Differential cell death programmes induced by silver dressings in vitro. Eur J Dermatol. 2008; 18(4):416–21. [PubMed: 18573715]
20. Cho Lee AR, Leem H, Lee J, Chan Park K. Reversal of silver sulfadiazine-impaired wound healing by epidermal growth factor. Biomaterials. 2005; 26(22):4670–6. [PubMed: 15722137]
21. Mintz EM, George DE, Hsu S. Silver sulfadiazine therapy in widespread bullous disorders: potential for toxicity. Dermatol Online J. 2008; 14(3)
22. Mendelsohn JD, Barrett CJ, Chan VV, Pal AJ, Mayes AM, Rubner MF. Fabrication of microporous thin films from polyelectrolyte multilayers. Langmuir. 2000; 16(11):5017–23.
23. Decher G. Fuzzy nanoassemblies: toward layered polymeric multicomposites. Science. 1997; 277(5330):1232–7.
24. Hammond PT. Recent explorations in electrostatic multilayer thin film assembly. Curr Opin Colloid Interface Sci. 1999; 4(6):430–42.
25. Lee D, Cohen RE, Rubner MF. Antibacterial properties of ag nanoparticle loaded multilayers and formation of magnetically directed antibacterial microparticles. Langmuir. 2005; 21(21):9651–9. [PubMed: 16207049]
26. Li Z, Lee D, Sheng X, Cohen RE, Rubner MF. Two-level antibacterial coating with both release-killing and contact-killing capabilities. Langmuir. 2006; 22(24):9820–3. [PubMed: 17106967]

27. Grunlan JC, Choi JK, Lin A. Antimicrobial behavior of polyelectrolyte multilayer films containing cetrimide and silver. Biomacromolecules. 2005; 6(2):1149–53. [PubMed: 15762688]
28. Yu DG, Lin WC, Yang MC. Surface modification of poly(l-lactic acid) membrane via layer-by-layer assembly of silver nanoparticle-embedded polyelectrolyte multilayer. Bioconjug Chem. 2007; 18(5):1521–9. [PubMed: 17688319]
29. Shi Z, Neoh KG, Zhong SP, Yung LYL, Kang ET, Wang W. *In vitro* antibacterial and cytotoxicity assay of multilayered polyelectrolyte-functionalized stainless steel. J Biomed Mater Res Part A. 2006; 76A(4):826–34.
30. Shiratori SS, Rubner MF. pH-Dependent thickness behavior of sequentially adsorbed layers of weak polyelectrolytes. Macromolecules. 2000; 33(11):4213–9.
31. Wang TC, Rubner MF, Cohen RE. Polyelectrolyte multilayer nanoreactors for preparing silver nanoparticle composites: controlling metal concentration and nanoparticle size. Langmuir. 2002; 18(8):3370–5.
32. Joly S, Kane R, Radzilowski L, Wang T, Wu A, Cohen RE, et al. Multilayer nanoreactors for metallic and semiconducting particles. Langmuir. 2000; 16(3):1354–9.
33. Logar M, Jancar B, Suvorov D, Kostanjsek R. In situ synthesis of Ag nanoparticles in polyelectrolyte multilayers. Nanotechnology. 2007; 18(32):325601–8.
34. Mendelsohn JD, Yang SY, Hiller J, Hochbaum AI, Rubner MF. Rational design of cytophilic and cytophobic polyelectrolyte multilayer thin films. Biomacromolecules. 2003; 4(1):96–106. [PubMed: 12523853]
35. Thompson MT, Berg MC, Tobias IS, Rubner MF, Van Vliet KJ. Tuning compliance of nanoscale polyelectrolyte multilayers to modulate cell adhesion. Biomaterials. 2005; 26(34):6836–45. [PubMed: 15972236]
36. Gupta JK, Tjipto E, Zelikin AN, Caruso F, Abbott NL. Characterization of the growth of polyelectrolyte multilayers formed at interfaces between aqueous phases and thermotropic liquid crystals. Langmuir. 2008; 24(10):5534–42. [PubMed: 18419143]
37. Choi J, Rubner MF. Influence of the degree of ionization on weak polyelectrolyte multilayer assembly. Macromolecules. 2005; 38(1):116–24.
38. Baldi C, Minoia C, Nucci AD, Capodaglio E, Manzo L. Effects of silver in isolated rat hepatocytes. Toxicol Lett. 1988; 41(3):261–8. [PubMed: 3376153]
39. Taylor PL, Ussher AL, Burrell RE. Impact of heat on nanocrystalline silver dressings: Part I: chemical and biological properties. Biomaterials. 2005; 26(35):7221–9. [PubMed: 16005512]
40. Coombs CJ, Wan AT, Masterton JP, Conyers RAJ, Pedersen J, Chia YT. Do burn patients have a silver lining? Burns. 1992; 18(3):179–84. [PubMed: 1642763]

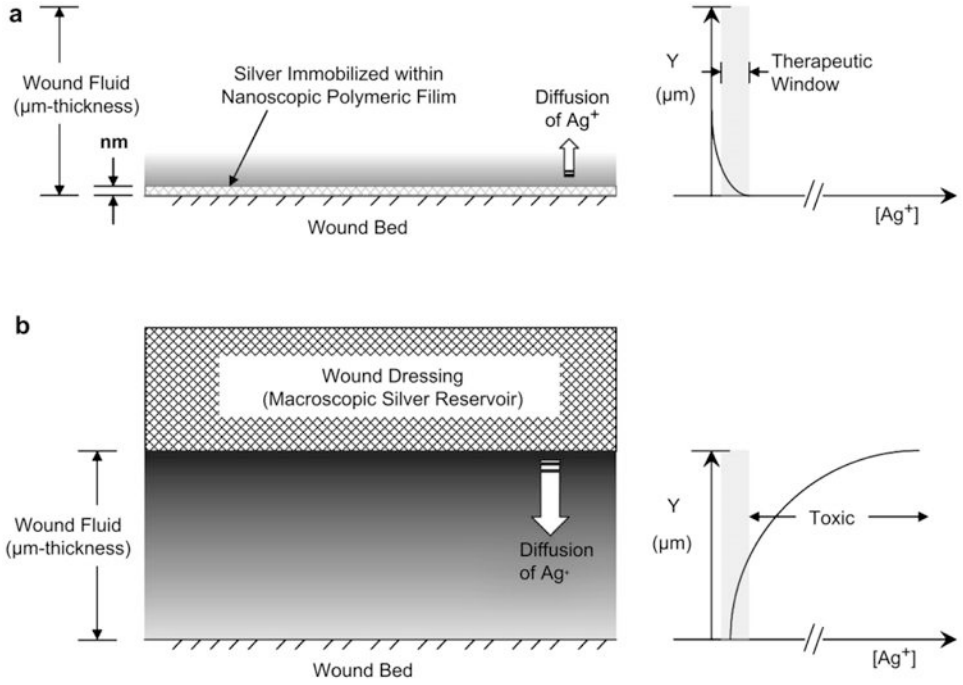

Fig. 1.

Schematic illustration of hypothesized concentration profiles of silver ions generated (a) by immobilization of silver nanoparticles within nanometer-thick polymeric films integrated into a wound bed, and (ii) by diffusion of silver ions from a macroscopic reservoir of silver (wound dressing) across wound fluid to a wound bed. The plot presented to the right of the schematic illustration in (a) shows that localization of silver nanoparticles to a wound bed can lead to a therapeutic window of silver ion concentrations at the surface of a wound bed without generating toxic concentrations of silver ions. In contrast, as illustrated in the plot presented to the right of (b), when delivering silver ions to a wound bed by diffusion from a macroscopic reservoir, toxic concentrations of silver ions are generated in wound fluid in order to achieve a therapeutic window of silver ion concentrations at the surface of a wound bed.

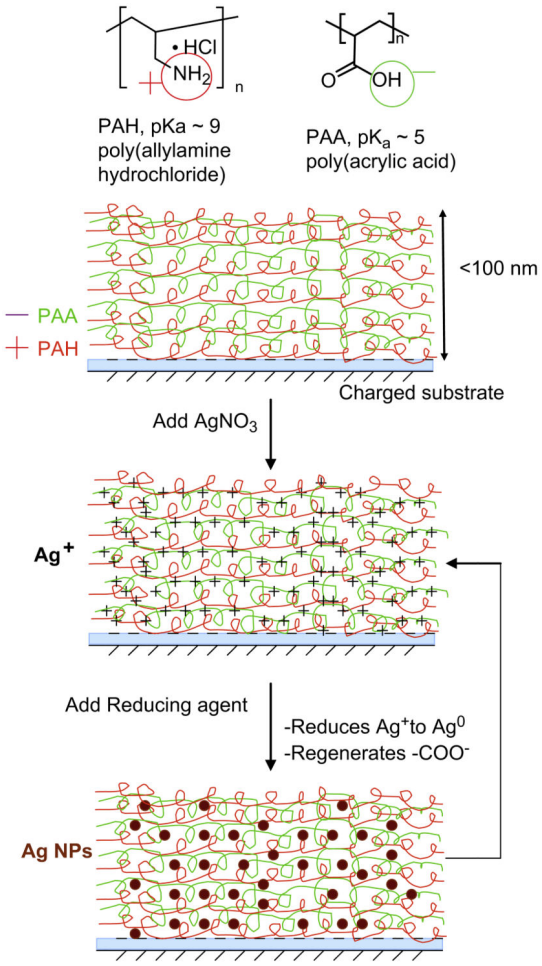

Fig. 2.

Schematic illustration of the layer-by-layer deposition of multilayers of PAH/PAA on a charged substrate. Post-assembly, the multilayer super-lattice is incubated with a solution of $AgNO_3$ in order to promote the exchange of the silver ions with protons of the carboxylic acid groups of PAA within the film. Subsequently, silver ions within the film are reduced to silver nanoparticles by a chemical reducing agent ($NaBH_4$). Chemical reduction of the silver ions to silver nanoparticles also regenerates the carboxylic groups within the film.

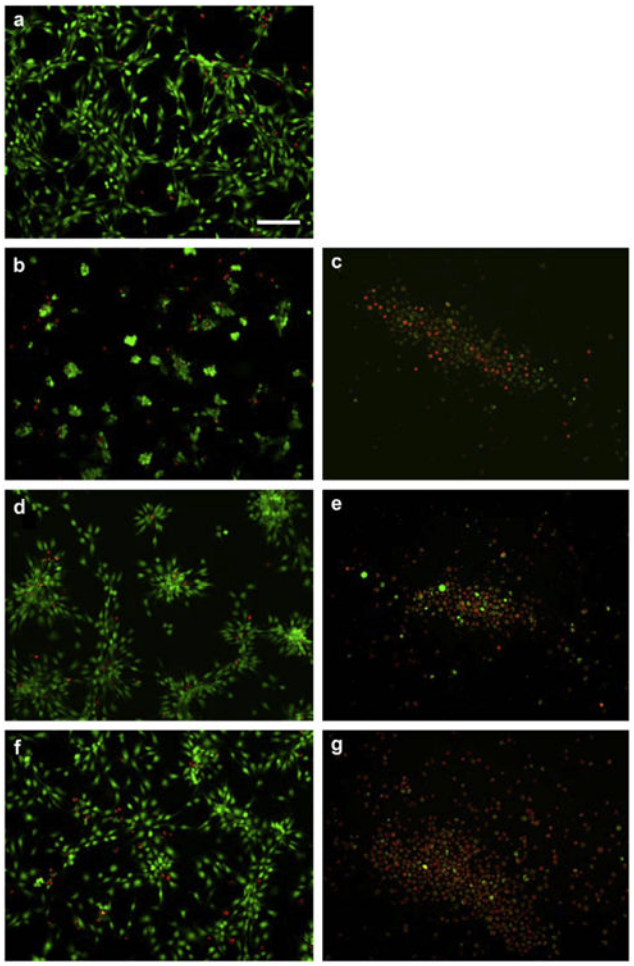

Fig. 3.

PEMs assembled under conditions leading to loadings of silver nanoparticles that are cytotoxic to NIH 3T3 mouse fibroblast cells. The figure shows NIH 3T3 cells after 24 h incubation on (a) an untreated glass surface, (b, d, f) PEM-(10.5 bilayers of $PAH_{7.5}/PAA_x$)-coated glass surfaces, without silver, (c, e, g) or PEM-coated surfaces with silver nanoparticles. Cells were labeled with live (green)/dead (red) fluorescent stains. PEMs were prepared using PAA solutions at pH 2.5 (b,c), or 3.5 (d,e) or 4.5 (f,g). Scale bar- 100 μm. See text for other details.

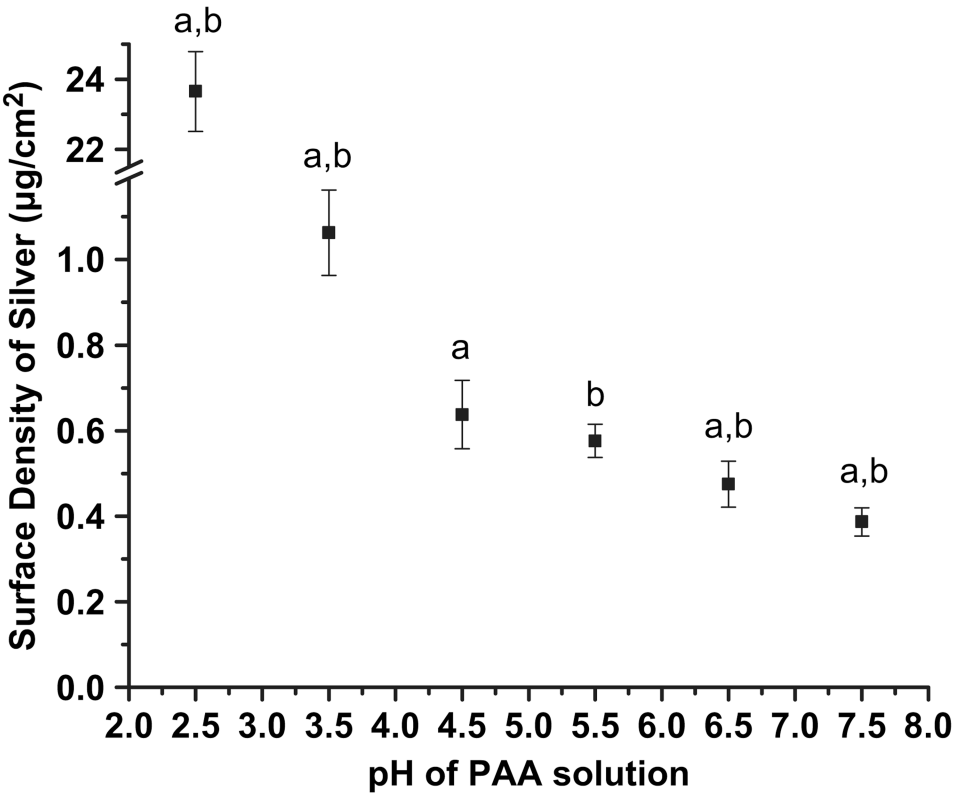

Fig. 4.

Amount of silver impregnated into PEMs (10.5 bilayers of $PAH_{7.5}/PAA_x$) can be tailored by varying the pH of the PAA solutions used to assemble the PEMs. The figure shows the loading of silver (µg/cm^2) within the PEMs prepared on 5 mm-diameter glass coverslips. Data points labeled with same letter of the alphabet are significantly different from each other, ($n \geq 3$, $p > 0.05$).

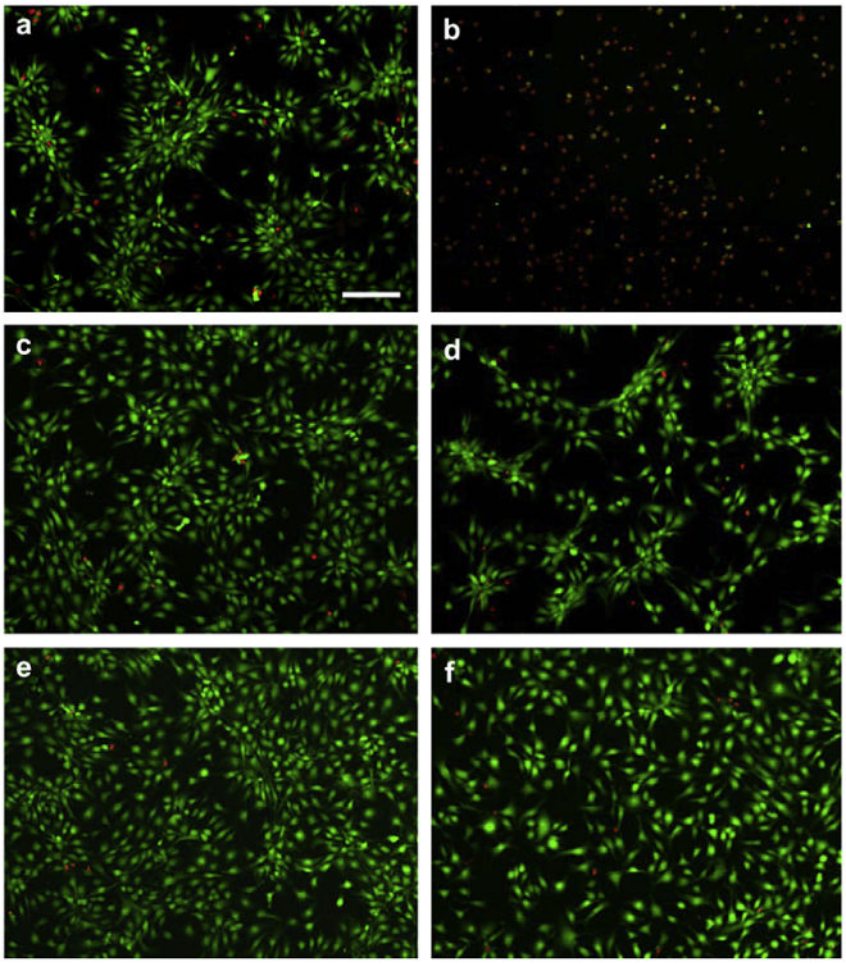

Fig. 5.

PEMs assembled under conditions leading to loadings of silver nanoparticles that are not cytotoxic to NIH 3T3 cells. The figure shows NIH 3T3 cells after 24 h incubation on (a, c, e) glass surfaces coated with PEMs (10.5 bilayers of $PAH_{7.5}/PAA_x$) without silver, or (b, d, f) or glass surfaces coated with PEMs impregnated with silver nanoparticles. The PEMs were prepared using PAA solutions at (a, b) pH 5.5, (c,d) 6.5, or (e,f) 7.5. The cells were labeled with live (green)/dead (red) fluorescent stains. Scale bar- 100 μm.

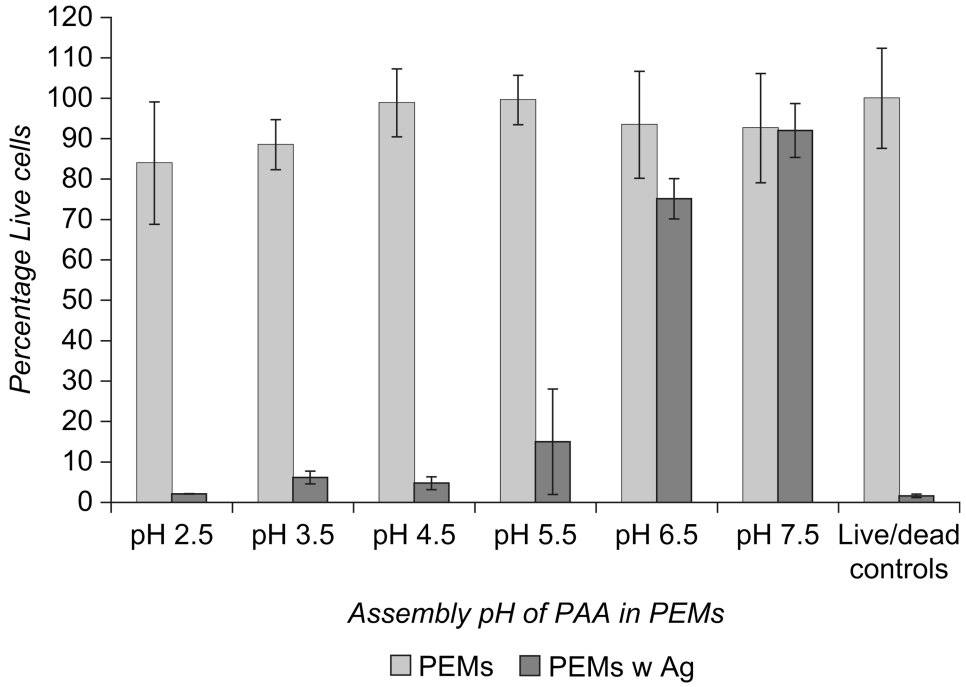

Fig. 6.

Viability of NIH 3T3 cells on PEM-coated glass surfaces impregnated with silver nanoparticles is silver-dose dependent. NIH 3T3 cells (1.5×10^4 per well) were incubated on PEM-coated glass coverslips placed in 96-well plates for 24 h and then labeled with live/dead fluorescent stains. PEMs were prepared using solutions of PAA with pH values ranging from 2.5 to 7.5 to vary the loading of silver. Data presented as mean ± S.D. with $n = 6$.

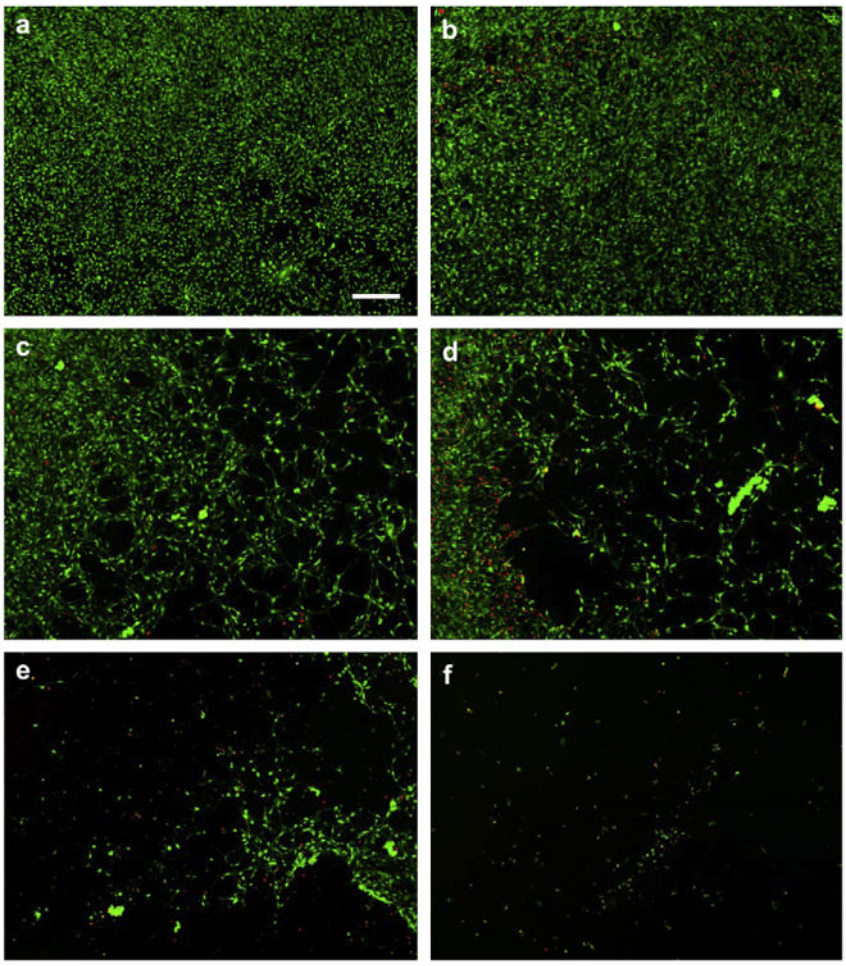

Fig. 7.

Cytotoxicity of NIH 3T3 cells to silver ions dissolved in growth media is dose-dependent. The Figure shows NIH 3T3 cells on glass coverslips after incubation for 36 h in serum-supplemented growth media to which $AgNO_3$ was added: (a) No silver, (b) 1 ppm, (c) 1.2 ppm, (d) 1.5 ppm, (e) 2 ppm, (f) 5 ppm. Cells were labeled with live (green)/dead (red) fluorescent stains. Scale-bar = 200 μm.

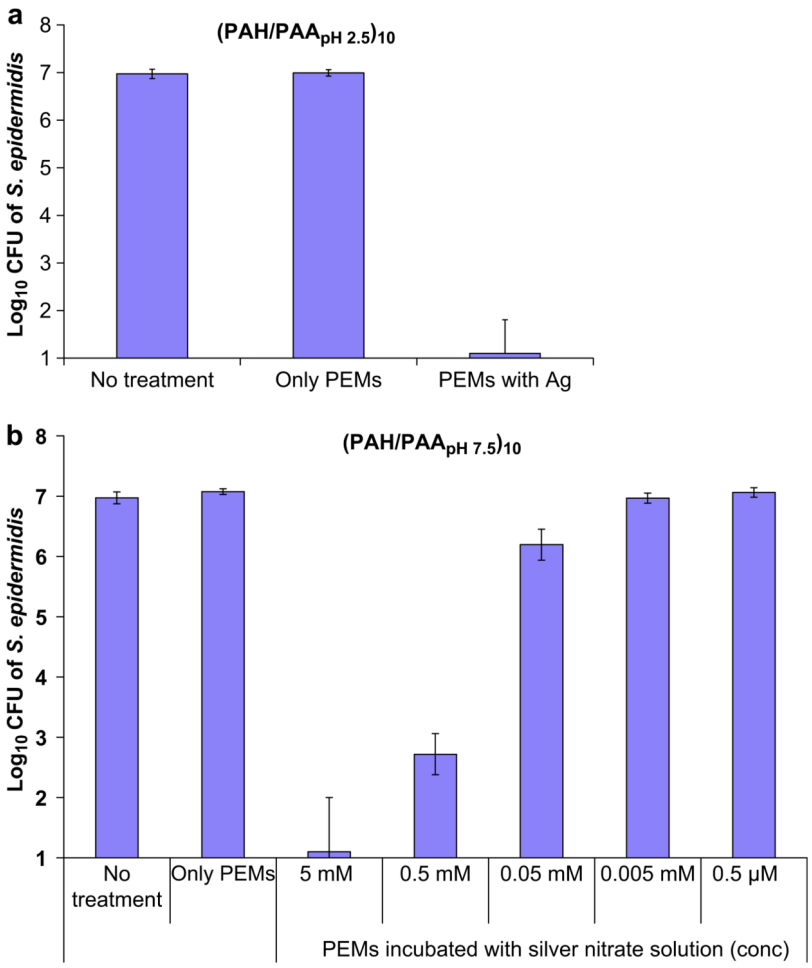

Fig. 8.

PEMs impregnated with as little as 0.39 ± 0.03 μg/cm^2 silver are bactericidal for *S. epidermidis*. PEM-coated glass coverslips were placed in 96-well plates and incubated with 10^7 CFU of S. *epidermidis* in 100 μl PBS buffer for 8 h with shaking (100 rpm) at 37 °C After incubation, bacteria were rinsed off the test wells and plated on agar to estimate viable cell counts (CFU/well). (a) PEMs assembled using PAA at pH 2.5 and impregnated with 23.6 ± 1.1 μg/cm^2 silver using a 5 mm silver nitrate solution. (b) PEMs assembled using PAA at pH 7.5 and impregnated with 0.39 ± 0.03 μg/cm^2 silver using a 5 mm silver nitrate solution. In addition, results are shown for PEMs were impregnated with concentrations of silver nitrate solutions that were less than 5.0 mm, as indicated on *x*-axis of the graph. The loadings of silver nanoparticles in the PEMs prepared using the low concentrations of silver were below the detection limit of ICP-ES. Overall, the data demonstrates silver-dose dependent bactericidal activity. Data presented as mean ± standard deviation (n = 3).